ASEC 2022

MDPI

Proceeding Paper

Effects of Guanidinium and Cesium Addition to $CH_3NH_3PbI_3$ Perovskite Photovoltaic Devices †

Takeo Oku [1,*], Iori Ono [1], Shoma Uchiya [1], Atsushi Suzuki [1], Masanobu Okita [2], Sakiko Fukunishi [2], Tomoharu Tachikawa [2] and Tomoya Hasegawa [2]

[1] Department of Materials Science, The University of Shiga Prefecture, 2500 Hassaka, Hikone, Shiga 522-8533, Japan; ov21ishimaji@ec.usp.ac.jp (I.O.); on21suchiya@ec.usp.ac.jp (S.U.); suzuki@mat.usp.ac.jp (A.S.)

[2] Osaka Gas Chemicals Co., Ltd., 5-11-61 Torishima, Konohana-ku, Osaka 554-0051, Japan; okita@ogc.co.jp (M.O.); fukunishi@ogc.co.jp (S.F.); t-tachikawa@ogc.co.jp (T.T.); hasegawa_tomoya@ogc.co.jp (T.H.)

* Correspondence: oku@mat.usp.ac.jp; Tel.: +81-749-28-8368

† Presented at the 3rd International Electronic Conference on Applied Sciences; Available online: https://asec2022.sciforum.net/.

Abstract: $CH_3NH_3PbI_3$ perovskite compounds are unstable in air due to the migration of CH_3NH_3. The purpose of the present work is to investigate the effects of addition of guanidinium $C(NH_2)_3$ (GA) and cesium (Cs) on $CH_3NH_3PbI_{3\ 3}$ perovskite solar cells. The addition of GA/Cs and the insertion of decaphenylpentasilane between the perovskite and hole transport layer improved the external quantum efficiency and short-circuit current density, and the conversion efficiencies were stable. First-principles calculations on the density of states and band structures showed reduction of the total energy by the GA addition.

Keywords: solar cell; guanidinium; cesium; polysilane; first principles calculation; photovoltaic device

Citation: Oku, T.; Ono, I.; Uchiya, S.; Suzuki, A.; Okita, M.; Fukunishi, S.; Tachikawa, T.; Hasegawa, T. Effects of Guanidinium and Cesium Addition to $CH_3NH_3PbI_3$ Perovskite Photovoltaic Devices. *Eng. Proc.* **2022**, *4*, x. https://doi.org/10.3390/xxxxx

Academic Editor(s):

Published: 1 December 2022

Publisher's Note: MDPI stays neutral with regard to jurisdictional claims in published maps and institutional affiliations.

Copyright: © 2022 by the authors. Submitted for possible open access publication under the terms and conditions of the Creative Commons Attribution (CC BY) license (https://creativecommons.org/licenses/by/4.0/).

1. Introduction

Although silicon is the most common solar cell material, the fabrication process is expensive. On the other hand, $CH_3NH_3PbI_3$ ($MAPbI_3$) compounds have been widely used for perovskite solar cells [1–5], and the $MAPbI_3$ perovskite compound have tunable band gaps and easy fabrication process with low cost. However, the $MAPbI_3$ compounds are unstable in the ordinary air due to the migration and desorption of CH_3NH_3 (MA) molecules [6–9]. To stabilize the perovskite structure, various kinds of cations such as formamidinium ($HC(NH_2)_2$, FA) [10–16], ethylammonium ($CH_3CH_2NH_3$, EA) [17,18], or guanidinium ($C(NH_2)_3$, GA) [19,20], which have larger ionic radii than methylammonium (CH_3NH_3, MA), have been introduced at the MA site, and the fabricated cells were stable to some extent. Introducing alkali metals such as cesium (Cs) [21–23], rubidium (Rb) [24–26], potassium (K) [27–30], and sodium (Na) [31–34], could also be effective because these metal elements do not desorb from the perovskite crystal.

Another approach to improve the stability of the perovskite solar cells is introducing polymeric materials such as polysilane [35–39]. Polysilanes have two important features that are *p*-type semiconductors and are stable at elevated temperatures above 300 °C.

The purpose of the present work is to fabricate $MAPbI_3$ perovskite solar cells added with GA and Cs, and to characterize the devices from experiments and first-principle calculation. In the present work, polysilane was also used both for protection of the perovskite layer and for hole transport [35,37].

2. Experimental Procedures

A fabrication process of photovoltaic devices of the present work is same as those of the previous works [40–42]. A TiO_2 compact layer was formed on the F-doped tin-oxide (FTO) substrates, and a mesoporous TiO_2 layer was formed on the compact TiO_2 layer. A perovskite layer with desired composition was formed on the mesoporous TiO_2 layer, and decaphenylcyclopentasilane (DPPS) which is one kind of polysilane was formed on the perovskite layer [35]. A layer of 2,2′,7,7′-tetrakis-(N,N-di(p-methoxyphenyl)amine)-9,9′-spirobifluorene (spiro-OMeTAD) was formed on the DPPS, and then gold (Au) metal electrodes were formed on the spiro-OMeTAD hole transport layer.

Current density voltage characteristics of the fabricated devices were measured under a solar simulating light source operated at 100 mW cm^{-2}. X-ray diffraction was used to investigate the microstructures of the devices, and first-principles calculation was also carried out to estimate the properties of the perovskite crystals [43–45].

3. Results and Discussion

To estimate the structural stability of perovskite compounds. a tolerance factor (t) is used [5,46,47] using the following equation:

$$t = \frac{r_A + r_X}{\sqrt{2}(r_B + r_X)}$$

where r_A, r_B, and r_X are the ionic radii of the A, B, and X ions for ABX_3 perovskite structures, respectively [5]. When the t-value is 1, the perovskite compound has a stable crystal structure with cubic symmetry. From the previous experimental studies on perovskite compounds, the perovskite structure could be formed in the range of $0.813 \leq t \leq 1.107$. Calculated t-factors of perovskite compounds are listed in Table 1. From this calculation, co-addition of GA and Cs could be one of the effective ways to stabilize the $MAPbI_3$ structure.

Table 1. Calculated t-factors of perovskite compounds.

Perovskite	t
$MAPbI_3$	0.912
$GAPbI_3$	1.039
$CsPbI_3$	0.851
$MA_{0.75}GA_{0.125}Cs_{0.125}PbI_3$	0.920
$MA_{0.845}GA_{0.125}Cs_{0.03}PbI_3$	0.926

Figure 1a is a structure model of $MA_{0.75}GA_{0.125}$ $Cs_{0.125}PbI_3$. MA molecules are substituted by GA and Cs, which are located diagonally. Based on this structure model, the physical properties could be predicted. Figure 1b is an electron diffraction pattern of $MA_{0.75}GA_{0.125}$ $Cs_{0.125}PbI_3$ calculated along [111]. Although the usual $MAPbI_3$ has 6-fold symmetry from the [111] incidence, the calculated electron diffraction pattern in Figure 1b shows 2-fold symmetry, which is due to the doped Cs and GA. Therefore, the high symmetry dimension of the space group of $Pm\bar{3}m$ for $MAPbI_3$ is reduced to lower symmetry.

From the first-principle calculations and experimental evaluations, addition of small amount of GA to $MAPbI_3$ is effective to stabilize the perovskite structure [48,49]. Although the addition of GA expands and distorts the crystal lattice of $MAPbI_3$, Cs would reduce the distortion of the lattice, which could lead to the stability of the perovskite crystal.

For the fabricated device with $MA_{0.845}GA_{0.125}Cs_{0.03}PbI_3$ perovskite compound, the high photoconversion efficiency was obtained, which would be in good agreement with the calculated results. The stability of the device at the room temperature was also good. Although several works on $GAPbI_3$ [50] and $CsPbI_3$ [51,52] compounds have been reported, few works have been reported on the co-addition of GA and Cs to $MAPbI_3$. The present work indicated the effectiveness of the co-addition of GA and Cs to the $MAPbI_3$ on the photovoltaic properties for perovskite solar cells.

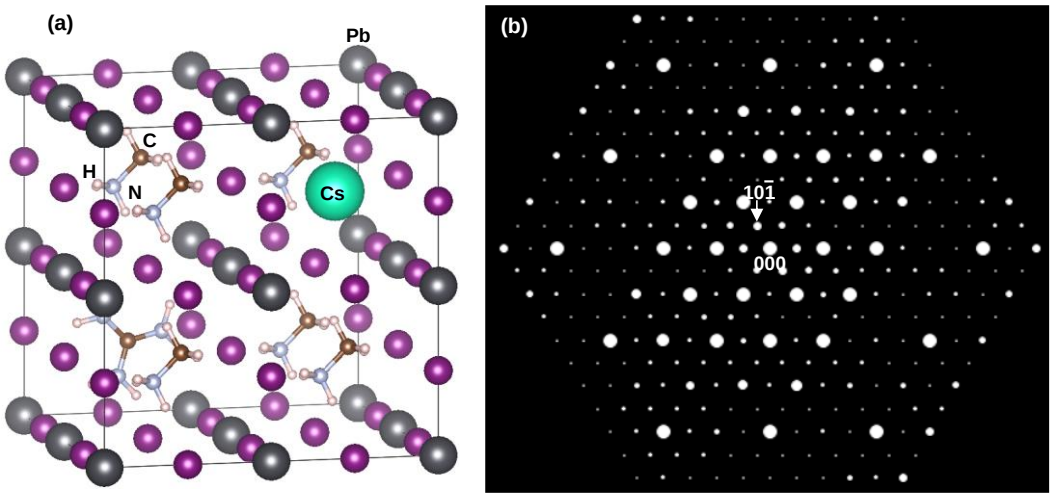

Figure 1. (**a**) Structure model and (**b**) calculated electron diffraction pattern along [111] of $MA_{0.75}GA_{0.125}Cs_{0.125}PbI_3$.

4. Conclusions

The effects of addition of guanidinium GA and Cs on $MAPbI_3$ perovskite solar cells were investigated. The co-addition of GA/Cs and the insertion of DPPS between the perovskite and spiro-OMeTAD improved the EQE, and the conversion efficiencies were stable. The calculated electron diffraction pattern of $MA_{0.75}GA_{0.125}Cs_{0.125}PbI_3$ showed reduction of the structural symmetry. First-principles calculations also showed reduction of the total energy by the GA addition, which indicated the stabilization by the addition.

Author Contributions: Conceptualization, T.O., I.O. and S.U.; Methodology, T.O., I.O., S.U. and A.S.; Formal Analysis, T.O., I.O., S.U. and A.S.; Investigation, T.O., I.O., S.U. and A.S.; Resources, M.O., S.F., T.T. and T.H.; Data Curation, T.O., I.O. and S.U.; Writing—Original Draft Preparation, T.O.; Writing—Review & Editing, T.O., I.O., S.U., A.S., M.O., S.F., T.T. and T.H.; Project Administration, T.O.; Funding Acquisition, T.O. All authors have read and agreed to the published version of the manuscript.

Funding: This research was partly funded by Japan Society for the promotion of Science as a Grant-in-Aid for Scientific Research (C) 21K04809.

Institutional Review Board Statement: Not applicable.

Informed Consent Statement: Not applicable.

Data Availability Statement: Data is contained within the article.

Conflicts of Interest: The authors declare no conflict of interest.

References

1. Bi, E.; Chen, H.; Xie, F.; Wu, Y.; Chen, W.; Su, Y.; Islam, A.; Grätzel, M.; Yang, X.; Han, L. Diffusion engineering of ions and charge carriers for stable efficient perovskite solar cells. *Nat. Commun.* **2017**, *8*, 15330. https://doi.org/10.1038/ncomms15330.
2. Tailor, N.K.; Abdi-Jalebi, M.; Gupta, V.; Hu, H.; Dar, M.I.; Li, G.; Satapathi, S. Recent progress in morphology optimization in perovskite solar cell. *J. Mater. Chem. A* **2020**, *8*, 21356–21386. https://doi.org/10.1039/d0ta00143k.
3. Liu, S.; Guan, Y.; Sheng, Y.; Hu, Y.; Rong, Y.; Mei, A.; Han, H. A review on additives for halide perovskite solar cells. *Adv. Energy Mater.* **2020**, *10*, 1902492. https://doi.org/10.1002/aenm.201902492.
4. Wang, P.; Zhao, Y.; Wang, T. Recent progress and prospects of integrated perovskite/organic solar cells. *Appl. Phys. Rev.* **2020**, *7*, 031303. https://doi.org/10.1063/5.0013912.
5. Oku, T. Crystal structures of perovskite halide compounds used for solar cells. *Rev. Adv. Mater. Sci.* **2020**, *59*, 264–305. https://doi.org/10.1515/rams-2020-0015.
6. Ono, L.K.; Liu, S.; Qi, Y. Reducing detrimental defects for high-performance metal halide perovskite solar cells. *Angew. Chem. Int. Ed.* **2020**, *59*, 6676–6698. https://doi.org/10.1002/anie.201905521.
7. Wang, R.; Mujahid, M.; Duan, Y.; Wang, Z.-K.; Xue, J.; Yang, Y. A review of perovskites solar cell stability. *Adv. Funct. Mater.* **2019**, *29*, 1808843. https://doi.org/10.1002/adfm.201808843.

8. Berhe, T.A.; Su, W.-N.; Chen, C.-H.; Pan, C.-J.; Cheng, J.-H.; Chen, H.-M.; Tsai, M.-C.; Chen, L.-Y.; Dubale, A.A.; Hwang, B.-J. Organometal halide perovskite solar cells: degradation and stability. *Energy Environ. Sci*. **2016**, *9*, 323–356. https://doi.org/10.1039/c5ee02733k.
9. Conings, B.; Drijkoningen, J.; Gauquelin, N.; Babayigit, A.; D'Haen, J.; D'Olieslaeger, L.; Ethirajan, A.; Verbeeck, J.; Manca, J.; Mosconi, E.; et al. Intrinsic thermal instability of methylammonium lead trihalide perovskite. *Adv. Energy Mater.* **2015**, *5*, 1500477. https://doi.org/10.1002/aenm.201500477.
10. Zhao, H.; Zhao, L.; Li, S.; Chu, Y.; Sun, Y.; Xie, B.; He, J.; Li, J. Recent Advances on the strategies to stabilize the α-phase of formamidinium based perovskite materials. *Crystals* **2022**, *12*, 573. https://doi.org/10.3390/cryst12050573.
11. Li, G.; Zhang, T.; Xu, F.; Zhao, Y. A facile deposition of large grain and phase pure α-$FAPbI_3$ for perovskite solar cells via a flash crystallization. *Mater. Today Energy* **2017**, *5*, 293–298. https://doi.org/10.1016/j.mtener.2017.07.010.
12. Jiang, Q.; Zhang, L.; Wang, H.; Yang, X.; Meng, J.; Liu, H.; Yin, Z.; Wu, J.; Zhang, X.; You, J. Enhanced electron extraction using SnO_2 for high-efficiency planar-structure $HC(NH_2)_2PbI_3$-based perovskite solar cells. *Nat. Energy* **2017**, *2*, 16177. https://doi.org/10.1038/nenergy.2016.177.
13. Yang, W.S.; Park, B.W.; Jung, E.H.; Jeon, N.J.; Kim, Y.C.; Lee, D.U.; Shin, S.S.; Seo, J.; Kim, E.K.; Noh, J.H.; et al. Iodide management in formamidinium-lead-halide-based perovskite layers for efficient solar cells. *Science* **2017**, *356*, 1376–1379. https://doi.org/10.1126/science.aan2301.
14. Lee, J.-W.; Dai, Z.; Lee, C.; Lee, H.M.; Han, T.-H.; De Marco, N.; Lin, O.; Choi, C.S.; Dunn, B.; Koh, J.; et al. Tuning molecular interactions for highly reproducible and efficient formamidinium perovskite solar cells via adduct approach. *J. Am. Chem. Soc.* **2018**, *140*, 6317–6324. https://doi.org/10.1021/jacs.8b01037.
15. Suzuki, A.; Taguchi, M.; Oku, T.; Okita, M.; Minami, S.; Fukunishi, S.; Tachikawa, T. Additive effects of methyl ammonium bromide or formamidinium bromide in methylammonium lead iodide perovskite solar cells using decaphenylcyclopentasilane. *J. Mater. Sci. Mater. Electron.* **2021**, *32*, 26449–26464. https://doi.org/10.1007/s10854-021-07023-w.
16. Suzuki, A.; Kato, M.; Ueoka, N.; Oku, T. Additive effect of formamidinium chloride in methylammonium lead halide compound-based perovskite solar cells. *J. Electron. Mater.* **2019**, *48*, 3900–3907. https://doi.org/10.1007/s11664-019-07153-2.
17. Wang, Y.; Zhang, T.; Li, G.; Xu, F.; Li, Y.; Yang, Y.; Zhao, Y. A mixed-cation lead iodide $MA_{1-x}EA_xPbI_3$ absorber for perovskite solar cells. *J. Energy Chem.* **2018**, *27*, 215–218. https://doi.org/10.1016/j.jechem.2017.09.027.
18. Nishi, K.; Oku, T.; Kishimoto, T.; Ueoka, N.; Suzuki, A. Photovoltaic characteristics of $CH_3NH_3PbI_3$ perovskite solar cells added with ethylammonium bromide and formamidinium iodide. *Coatings* **2020**, *10*, 410. https://doi.org/10.3390/coatings10040410.
19. Jodlowski, A.D.; Roldán-Carmona, C.; Grancini, G.; Salado, M.; Ralaiarisoa, M.; Ahmad, S.; Koch, N.; Camacho, L.; Miguel, G.; Nazeeruddin, M. Large guanidinium cation mixed with methylammonium in lead iodide perovskites for 19% efficient solar cells. *Nat. Energy* **2017**, *2*, 972–979. https://doi.org/10.1038/s41560-017-0054-3.
20. Kishimoto, T.; Suzuki, A.; Ueoka, N.; Oku, T. Effects of guanidinium addition to $CH_3NH_3PbI_{3-x}Cl_x$ perovskite photovoltaic devices. *J. Ceram. Soc. Jpn.* **2019**, *127*, 491–497. https://doi.org/10.2109/jcersj2.18214.
21. Song, J.; Xie, H.; Lim, E.L.; Hagfeldt, A.; Bi, D. Progress and perspective on inorganic $CsPbI_2Br$ perovskite solar cells *Adv. Energy Mater.* **2022**, 2201854. https://doi.org/10.1002/aenm.202201854.
22. Ueoka, N.; Oku, T.; Suzuki, A. Additive effects of alkali metals on Cu-modified $CH_3NH_3PbI_{3-\delta}Cl_\delta$ photovoltaic devices. *RSC Adv.* **2019**, *9*, 24231. https://doi.org/10.1039/C9RA03068A.
23. Li, N.; Luo, Y.; Chen, Z.; Niu, X.; Zhang, X.; Lu, J.; Kumar, R.; Jiang, J.; Liu, H.; Guo, X.; et al. Microscopic Degradation in Formamidinium-Cesium Lead Iodide Perovskite Solar Cells under Operational Stressors. *Joule* **2020**, *4*, 8. https://doi.org/10.16/j.joule.2020.06.005.
24. Saliba, M.; Matsui, T.; Domanski, K.; Seo, J.-Y.; Ummadisingu, A.; Zakeeruddin, M.S.; Correa-Baena, J.-P.; Tress, R.W.; Abate, A.; Hagfeldt, A.; et al. Incorporation of rubidium cations into perovskite solar cells improves photovoltaic performance. *Science* **2016**, *354*, 206. https://doi.org/10.1126/science.aah5557.
25. Ueoka, N.; Oku, T.; Suzuki, A. Effects of doping with Na, K, Rb, and formamidinium cations on $(CH_3NH_3)_{0.99}Rb_{0.01}Pb_{0.99}Cu_{0.01}I_{3-x}(Cl, Br)_x$ perovskite photovoltaic cells. *AIP Adv.* **2020**, *10*, 125023. https://doi.org/10.1063/5.0029162.
26. Suzuki, A.; Oe, M.; Oku, T. Fabrication and characterization of Ni-, Co-, and Rb-incorporated $CH_3NH_3PbI_3$ perovskite solar cells. *J. Electron. Mater.* **2021**, *50*, 1980–1995. https://doi.org/10.1007/s11664-021-08759-1.
27. Machiba, H.; Oku, T.; Kishimoto, T.; Ueoka, N.; Suzuki, A. Fabrication and evaluation of K-doped $MA_{0.8}FA_{0.1}K_{0.1}PbI_3$(Cl) perovskite solar cells. *Chem. Phys. Lett.* **2019**, *730*, 117–123. https://doi.org/10.1016/j.cplett.2019.05.050.
28. Kandori, S.; Oku, T.; Nishi, K.; Kishimoto, T.; Ueoka, N.; Suzuki, A. Fabrication and characterization of potassium- and formamidinium-added perovskite solar cells. *J. Ceram. Soc. Jpn.* **2020**, *128*, 805–811. https://doi.org/10.2109/jcersj2.20090.
29. Oku, T.; Kandori, S.; Taguchi, M.; Suzuki, A.; Okita, M.; Minami, S.; Fukunishi, S.; Tachikawa, T. Polysilane-inserted methylammonium lead iodide perovskite solar cells doped with formamidinium and potassium. *Energies* **2020**, *13*, 4776. https://doi.org/10.3390/en13184776.
30. Enomoto, A.; Suzuki, A.; Oku, T.; Okita, M.; Fukunishi, S.; Tachikawa, T.; Hasegawa, T. Effects of Cu, K and guanidinium addition to $CH_3NH_3PbI_3$ perovskite solar cells. *J. Electron. Mater.* **2022**, *51*, 4317–4328. https://doi.org/10.1007/s11664-022-09688-3.
31. Ueoka, N.; Oku, T. Effects of co-addition of sodium chloride and copper (II) bromide to mixed-cation mixed-halide perovskite photovoltaic devices. *ACS Appl. Energy Mater.* **2020**, *3*, 7272–7283. https://doi.org/10.1021/acsaem.0c00182.

32. Suzuki, A.; Kitagawa, K.; Oku, T.; Okita, M.; Fukunishi, S.; Tachikawa, T., Additive effects of copper and alkali metal halides into methylammonium lead iodide perovskite solar cells, *Electron. Mater. Lett.* **2022**, *18*, 176–186. https://doi.org/10.1007/s13391-021-00325-5.
33. Okumura, R.; Oku, T.; Suzuki, A.; Okita, M.; Fukunishi, S.; Tachikawa, T.; Hasegawa, T. Effects of adding alkali metals and organic cations to Cu-based perovskite solar cells. *Appl. Sci.* **2022**, *12*, 1710. https://doi.org/10.3390/app12031710.
34. Suzuki, A.; Miyamoto, Y.; Oku, T.; Electronic structures, spectroscopic properties, and thermodynamic characterization of sodium- or potassium-incorporated $CH_3NH_3PbI_3$ by first-principles calculation, *J. Mater. Sci.* **2020**, *55*, 9728–9738. https://doi.org/10.1007/s10853-020-04511-y.
35. Oku, T.; Taguchi, M.; Suzuki, A.; Kitagawa, K.; Asakawa, Y.; Yoshida, S.; Okita, M.; Minami, S.; Fukunishi, S.; Tachikawa, T. Effects of polysilane addition to chlorobenzene and high temperature annealing on $CH_3NH_3PbI_3$ perovskite photovoltaic devices. *Coatings* **2021**, *11*, 665. https://doi.org/10.3390/coatings11060665.
36. Taguchi, M.; Suzuki, A.; Oku, T.; Fukunishi, S.; Minami, S.; Okita, M. Effects of decaphenylcyclopentasilane addition on photovoltaic properties of perovskite solar cells. *Coatings* **2018**, *8*, 461. https://doi.org/10.3390/coatings8120461.
37. Oku, T.; Nakagawa, J.; Iwase, M.; Kawashima, A.; Yoshida, K.; Suzuki, A.; Akiyama, T.; Tokumitsu, K.; Yamada, M.; Nakamura, M. Microstructures and photovoltaic properties of polysilane-based solar cells. *Jpn. J. Appl. Phys.* **2013**, *52*, 04CR07. https://doi.org/10.7567/JJAP.52.04CR07.
38. Oku, T.; Nomura, J.; Suzuki, A.; Tanaka, H.; Fukunishi, S.; Minami, S.; Tsukada, S. Fabrication and characterization of $CH_3NH_3PbI_3$ perovskite solar cells added with polysilanes. *Int. J. Photoenergy* **2018**, *2018*, 8654963. https://doi.org/10.1155/2018/8654963.
39. Taguchi, M.; Suzuki, A.; Oku, T.; Ueoka, N.; Minami, S.; Okita, M. Effects of annealing temperature on decaphenylcyclopentasilane-inserted $CH_3NH_3PbI_3$ perovskite solar cells. *Chem. Phys. Lett.* **2019**, *737*, 136822. https://doi.org/10.1016/j.cplett.2019.136822.
40. Oku, T.; Zushi, M.; Imanishi, Y.; Suzuki, A.; Suzuki, K. Microstructures and photovoltaic properties of perovskite-type $CH_3NH_3PbI_3$ compounds. *Appl. Phys. Express* **2014**, *7*, 121601. https://doi.org/10.7567/APEX.7.121601.
41. Ueoka, N.; Oku, T. Stability characterization of PbI_2-added $CH_3NH_3PbI_{3-x}Cl_x$ photovoltaic devices. *ACS Appl. Mater. Interfaces* **2018**, *10*, 44443−44451. https://doi.org/10.1021/acsami.8b16029.
42. Oku, T.; Ohishi, Y.; Ueoka, N. Highly (100)-oriented $CH_3NH_3PbI_3$(Cl) perovskite solar cells prepared with NH_4Cl using an air blow method. *RSC Adv.* **2018**, *8*, 10389–10395. https://doi.org/10.1039/c7ra13582c.
43. Suzuki, A.; Kishimoto, K.; Oku, T.; Okita, M.; Fukunishi, S.; Tachikawa, Additive effect of lanthanide compounds into perovskite layer on photovoltaic properties and electronic structures. *Synth. Met.* **2022**, *287*, 117092. https://doi.org/10.1016/j.synthmet.2022.117092.
44. Suzuki, A.; Oku, T. Effects of mixed-valence states of Eu-doped $FAPbI_3$ perovskite crystals studied by first-principles calculation, *Mater. Adv.* **2021**, *2*, 2609–2616. https://doi.org/10.1039/D0MA00994F.
45. Suzuki, A.; Oku, T. First-principles calculation study of electronic structures of alkali metals (Li, K, Na and Rb)-incorporated formamidinium lead halide perovskite compounds, *Appl. Surf. Sci.* **2019**, *483*, 912–921. https://doi.org/10.1016/j.apsusc.2019.04.049.
46. Li, Z.; Yang, M.; Park, J.S.; Wei, S.H.; Berry, J.J.; Zhu, K. Perovskite structures by tuning tolerance factor: Formation of formamidinium and cesium lead iodide solid-state alloys. *Chem. Mater.* **2016**, 28, 284–292. https://doi.org/10.1021/acs.chemmater.5b04107.
47. Tanaka, H.; Oku, T.; Ueoka, N. Structural stabilities of organic-inorganic perovskite crystals. *Jpn. J. Appl. Phys*. **2018,** *57*, 08RE12. https://doi.org/10.7567/JJAP.57.08RE12.
48. Kishimoto, T.; Oku, T.; Suzuki, A.; Ueoka, N. Additive effects of guanidinium iodide on $CH_3NH_3PbI_3$ perovskite solar cells. *Phys. Status Solidi A* **2021**, *218*, 2100396. https://doi.org/10.1002/pssa.202100396.
49. Ono, I.; Oku, T.; Suzuki, A.; Asakawa, Y.; Terada, S.; Okita, M.; Fukunishi, S.; Tachikawa, T. Fabrication and characterization of $CH_3NH_3PbI_3$ solar cells with added guanidinium and inserted with decaphenylpentasilane, *Jpn. J. Appl. Phys.* **2022**, *61*, SB1024. https://doi.org/10.35848/1347-4065/ac2661.
50. Kim, Y.; Nandi, P.; Lee, D.; Shin, H. Stabilization of 3-D trigonal phase in guanidinium ($C(NH_2)_3$) lead triiodide ($GAPbI_3$) films. *Appl. Surf. Sci.* **2021**, *542*, 148575, https://doi.org/10.1016/j.apsusc.2020.148575.
51. Suzuki, A.; Oku, T. Electronic structures and magnetic properties of transition metal doped $CsPbI_3$ perovskite compounds by first-principles calculation. *Phys. Solid State*, **2019**, *61*, 1074–1085. https://doi.org/10.1134/S1063783419060258.
52. Liu, D.; Shao, Z.; Li, C.; Pang, S.; Yan, Y.; Cui, G. Structural properties and stability of inorganic $CsPbI_3$ perovskites. *Small Struct.* **2021**, *2*, 2000089. https://doi.org/10.1002/sstr.202000089.